Inorganic Chemistry
Article

Inorg. Chem. **2010**, *49*, 4355–4361 **4355**
DOI: 10.1021/ic1003287

Field Induced 4f5d $[Re(salen)]_2O_3[Dy(hfac)_3(H_2O)]_2$ Single Molecule Magnet

Fabrice Pointillart,*,†,‡ K. Bernot,†,§ R. Sessoli,*,† and D. Gatteschi†

†*L.A.M.M, Department of Chemistry and INSTM Research Unit, Università di Firenze, Via Della Lastruccia 3, 50019 Sesto Fiorentino, Italy,* ‡*Sciences Chimiques de Rennes, UMR 6226 CNRS-UR1, Equipe ≪ Organométalliques et Matériaux Inorganiques ≫, Université Rennes 1, 263 Avenue du Général Leclerc, 35042 Rennes Cedex, France, and* §*Université Européenne de Bretagne, INSA, SCR, UMR 6226, F-35708 Rennes, France*

Received February 18, 2010

The reaction between the mononuclear [ReO(salen)(OMe)] ($salen^{2-}$ = *N,N′*-ethan-1,2-diylbis(salicylidenamine) dianion) and $Dy(hfac)_3 \cdot 2H_2O$ ($hfac^-$ = 1,1,1,5,5,5-hexafluoroacetylacetonate anion) complexes lead to the formation of a compound with the formula $\{[Re(salen)]_2O_3[Dy(hfac)_3(H_2O)]_2\}(CHCl_3)_2(CH_2Cl_2)_2$ noted (**Dy_2Re_2**). This compound has been characterized by single crystal and powder X-ray diffraction and has been found isostructural to the Y(III) derivative (**Y_2Re_2**) that we previously reported. The cyclic voltammetry demonstrates the redox activity of the system. The characterization of both static and dynamic magnetic properties is reported. Static magnetic data has been analyzed after the cancellation of the crystal field contribution by two different methods. Weak ferromagnetic exchange interactions between the Dy(III) ions are highlighted. The compound **Dy_2Re_2** displays slow relaxation of the magnetization when an external magnetic field is applied. Alternating current susceptibility shows a thermally activated behavior with pre-exponential factors of 7.13 ($\pm$0.10) $\times$ 10^{-6} and 5.76 ($\pm$0.27) $\times$ 10^{-7} s, and energy barriers of 4.19 ($\pm$0.02) and 8.52 ($\pm$0.55) K respectively for low and high temperature regimes.

Introduction

The exploration for high performance molecular magnets is currently an important research subject for both physicist and chemist communities. In particular, zero-dimensional complexes like Single Molecule Magnets (SMMs)[1] have been intensively investigated because of their potential applications for future devices. Recently, lanthanides-based SMMs have added to the library since trivalent rare-earth ions present many advantages, as compared to transition metal ions. Indeed, their large spins and pronounced spin−orbit coupling may result in strong Ising-type magnetic anisotropy.[2] The most popular lanthanide ions used for this magnetic peculiarity are certainly Dy(III) and Tb(III) ions. Many mono, bi-, and trinuclear complexes built with these ions have been reported as SMMs.[3] Moreover, to increase the spin ground state of such complexes, 3d metal ions can be associated to these ions to enhance the intramolecular magnetic exchange interactions in complexes.[4] As a last development, substitution of 3d ions by 4d or 5d ions may lead to an increase of the exchange interactions because of the diffuse orbital for second and third transition metal series and some 4d or 5d-based SMMs have been recently reported.[5]

Schiff-base Rhenium complexes are an example of a potential 5d precursor, and were mainly studied for their application in nuclear medicine where Rhenium is used as a non-radioactive model for technetium.[6] In $[Re(salen)]_2O_3$, ($salen^{2-}$ = *N,N′*-ethan-1,2-diylbis(salicylidenamine) dianion),

*To whom correspondence should be addressed. E-mail: fabrice.pointillart@univ-rennes1.fr.

(1) Ritter, S. K. *Chem. Eng. News* **2004**, *82*, 29.
(2) Carlin, R. L. *Magnetochemistry*; Springer: Berlin, 1986.
(3) For example: (a) Ishikawa, N.; Sugita, M.; Ishikawa, T.; Koshihara, S.; Kaizu, Y. *J. Am. Chem. Soc.* **2003**, *125*, 8694. (b) Ishikawa, N.; Sugita, M.; Wernsdorfer, W. *J. Am. Chem. Soc.* **2005**, *127*, 3650. (c) Tang, J.; Hewitt, I.; Madhu, N. T.; Chastanet, G.; Wernsdorfer, W.; Anson, C. E.; Benelli, C.; Sessoli, R.; Powell, A. K. *Angew. Chem.* **2006**, *118*, 1761. *Angew. Chem., Int. Ed.* **2006**, *45*, 1729. (d) Lin, P.-H.; Burchell, T.-J.; Clérac, R.; Murugesu, M. *Angew. Chem., Int. Ed.* **2008**, *47*, 8848. (e) Ishikawa, N. *Polyhedron* **2007**, *26*, 2147 and references herein.
(4) (a) Osa, S.; Kido, T.; Matsumoto, N.; Re, N.; Pochaba, A.; Mrozinski, J. *J. Am. Chem. Soc.* **2004**, *126*, 420. (b) Zaleski, C. M.; Depperman, E. C.; Kampf, J. W.; Kirk, M. L.; Pecoraro, V. L. *Angew. Chem.* **2004**, *116*, 4002. *Angew. Chem., Int. Ed.* **2004**, *43*, 3912. (c) Mishra, A.; Wernsdorfer, W.; Parsons, S.; Christou, G.; Brechin, E. K. *Chem. Commun.* **2005**, 2086. (d) Mori, F.; Nyui, T.; Ishida, T.; Nogami, T.; Choi, K.-Y.; Nojiri, H. *J. Am. Chem. Soc.* **2006**, *128*, 1440. (e) Costes, J. P.; Dahan, F.; Wernsdorfer, W. *Inorg. Chem.* **2006**, *45*, 5. (f) Pointillart, F.; Bernot, K.; Sessoli, R.; Gatteschi, D. *Chem.—Eur. J.* **2006**, *13*, 2602. (g) Wang, Y.; Li, X.-L.; Wang, T.-W.; Song, Y.; You, X.-Z. *Inorg. Chem.* **2010**, *49*, 969.
(5) (a) Martinez-Lillo, J.; Armentano, D.; De Munno, G.; Wernsdorfer, W.; Julve, M.; Lloret, F.; Faus, J. *J. Am. Chem. Soc.* **2006**, *128*, 14218. (b) Martinez-Lillo, J.; Delgado, F. S.; Ruiz-Pérez, C.; Lloret, F.; Julve, M.; Faus, J. *Inorg. Chem.* **2007**, *46*, 3523. (c) Freedman, D. E.; Jenkins, D. M.; Lavarone, A. T.; Long, J. R. *J. Am. Chem. Soc.* **2008**, *130*, 2884.
(6) (a) Middleton, A. R.; Masters, A. F.; Wilkinson, G. J. *J. Chem. Soc., Dalton Trans.* **1979**, 542. (b) Bandoli, G.; Nicolini, M.; Mazzi, U.; Refosco, F. *J. Chem. Soc., Dalton Trans.* **1984**, 2505. (c) Jurrisson, S.; Lindoy, L. F.; Dancey, K. P.; McPertlin, M.; Tasker, P. A.; Uppal, D. K.; Deutscher, E. *Inorg. Chem.* **1984**, *23*, 227. (d) Marchi, A.; Duatti, A.; Rossi, R.; Magon, L.; Mazzi, U.; Pasquetto, A. *Inorg. Chim. Acta* **1984**, *81*, 15. (e) Tisato, F.; Refosco, F.; Mazzi, U.; Bandoli, G.; Dolmella, A. *Inorg. Chim. Acta* **1989**, *164*, 127. (f) Tisato, F.; Refosco, F.; Mazzi, U.; Bandoli, G.; Dolmella, A. *Inorg. Chim. Acta* **1991**, *189*, 97.

Published on Web 04/12/2010

the surprising reactivity of the Re=O group gave rise to tetranuclear complexes in which two lanthanides ions were connected through the O=Re−O−Re=O bridge.[7] Along this family of compounds, $\{[Re(salen)]_2O_3[Y(hfac)_3(H_2O)]_2\}(CHCl_3)_2(CH_2Cl_2)_2$ (Y_2Re_2) was the first that we reported since it was the only compound for which we were able to obtain X-ray quality single crystals. The goal was then to obtain the first ever 4f-5d paramagnetic complex. Such compound may indeed have interesting magnetic properties and, given the strong anisotropy of the ions used, have a possible SMM behavior. This implies the use of paramagnetic lanthanides ions and then the conversion of the diamagnetic Re(V) into a paramagnetic form of Rhenium upon oxidation to Re(VI) or reduction to Re(IV). While the former has given promising results in oxygen atom transfer,[8] the latter is known for its magnetic anisotropy.[5]

We report here the second step of this strategy, which is the coordination of paramagnetic and anisotropic lanthanide ions on the diamagnetic O=Re(V)−O−Re(V)=O bridge. The $\{[Re(salen)]_2O_3[Ln(hfac)_3(H_2O)]_2\}(CHCl_3)_2(CH_2Cl_2)_2$ (**Ln_2Re_2**) complexes possess two main characteristics; (i) the short O=Re−O−Re=O bridge allows to investigate the capability of this diamagnetic central unit to transmit a sizable magnetic interaction between the external paramagnetic units, (ii) the presence of an inversion center in the central oxygen atom made the two lanthanide ions symmetry related and thus maximizes the effect of their magnetic anisotropy since the two Ising axes are collinear. This may be a significant benefit for the dynamic magnetic properties of the complex.[4f,9]

We report here the characterization of $\{[Re(salen)]_2O_3[Dy(hfac)_3(H_2O)]_2\}(CHCl_3)_2(CH_2Cl_2)_2$ (**Dy_2Re_2**) and Dysprosium doped $\{[Re(salen)]_2O_3[Dy_xY_{2-x}(hfac)_3(H_2O)]_2\}(CHCl_3)_2(CH_2Cl_2)_2$ (**$Dy_xY_{2-x}Re_2$**) by X-ray powder diffraction, energy-dispersive spectrometry (EDS) analysis, cyclic voltammetry, static and dynamic magnetic measurements.

Experimental Section

Synthesis. General Procedures and Materials. The precursors $Ln(hfac)_3\cdot 2H_2O$ (For Ln(III) = Y, Gd and Dy)[10] ($hfac^-$ = 1,1,1,5,5,5-hexafluoroacetylacetonate anion) and [ReO(salen)(OMe)][11] complex ($salen^{2-}$ = *N*,*N*′-ethan-1,2-diylbis(salicylidenamine) dianion) were synthesized following previously reported methods. All other reagents were purchased from Aldrich Co. Ltd. and were used without further purification.

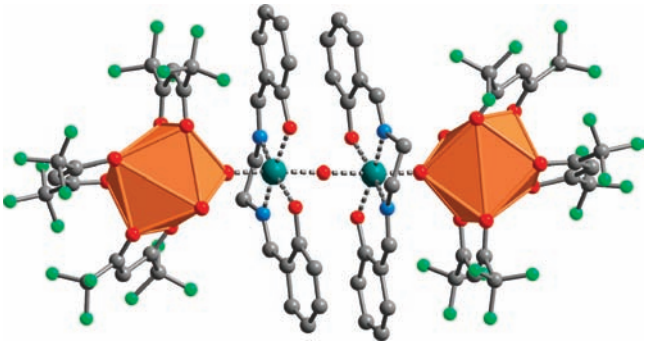

Figure 1. View of the crystal structure of $\{[Re(salen)]_2O_3[Ln(hfac)_3(H_2O)]_2\}(CHCl_3)_2(CH_2Cl_2)_2$ (**Ln_2Re_2**) family with the coordination polyhedron of the terminal Ln(III) ions. Hydrogen atoms have been omitted for clarity.

$\{[Re(salen)]_2O_3[Dy(hfac)_3(H_2O)]_2\}(CHCl_3)_2(CH_2Cl_2)_2$ latter named (Re_2Dy_2). A 491 mg portion of [ReO(salen)(OMe)] (1 mmol) was dissolved in 50 mL of $CHCl_3$ at 50 °C under aerobic atmosphere. The slow evaporation of the resulting green solution leads to a crystalline green powder of $\{[Re(salen)]_2O_3\}$. On one hand, 94.4 mg of $\{[Re(salen)]_2O_3\}$ (0.1 mmol) was dissolved in a mixture of CH_2Cl_2 and $CHCl_3$ (1:1 in volume, 20 mL). On the other hand a solution of 163.9 mg of $Dy(hfac)_3\cdot 2H_2O$ (0.2 mmol) in $CHCl_3$ (10 mL) was prepared. It was then added to the $\{[Re(salen)]_2O_3\}$ solution at 40 °C. The resulting mixture was stirred at 40 °C during 30 min. Red-brown needles were obtained by slow evaporation of the solution after one night. Single crystals were found to become very quickly amorphous by loss of the solvent molecules. They thus have to be conserved in the mother solution or in a tiny fiber glass. Anal. Calcd (%) for $C_{66}H_{44}N_4O_{22}Cl_{10}F_{36}Re_2Dy_2$: C 26.59, H 1.49, N 1.88; found: C 29.56, H 1.73, N 2.22. Discrepancies between calculated and observed values are due to the loss of solvent molecules.

$\{[Re(salen)]_2O_3[Dy_x(hfac)_3\ Y_{2-x}(hfac)_3\ (H_2O)]_2\}(CHCl_3)_2(CH_2Cl_2)_2$ latter named ($Dy_xY_{2-x}Re_2$). A similar procedure as for Dy_2Re_2 was used starting from 98.2 mg of $\{[Re(salen)]_2O_3\}$ (0.1 mmol). The heterolanthanides based solution was prepared with 8.2 mg of $Dy(hfac)_3\cdot 2H_2O$ (0.01 mmol) and 67.1 mg of $Y(hfac)_3\cdot 2H_2O$ (0.09 mmol) in $CHCl_3$ (10 mL). As for Dy_2Re_2, single crystals were found to become very quickly amorphous by loss of the solvent molecules. They were conserved in a very small amount of pure $CHCl_3$ and not in the mother solution to avoid the deposition of the excess of lanthanide that does not coordinate to the Re-based moiety. In fact, this could hamper the accurate determination of the doping rate of the crystals. Anal. Calcd (%) for $C_{66}H_{44}N_4O_{22}Cl_{10}F_{36}Re_2Y_{1.72}Dy_{0.28}$: C 27.77, H 1.55, N 1.96; found: C 30.01, H 1.79, N 2.34. Discrepancies between calculated and observed values are due to the loss of solvent molecules.

Crystallography. The crystal structure of Re_2Y_2, depicted in Figure 1, has already been reported.[7] Cell parameters determination for Re_2Dy_2 and $Dy_xY_{2-x}Re_2$ were performed on the same apparatus.

X-ray powder diffraction diagrams were recorded using a Panalytical X'Pert Pro diffractometer equipped with an X'celerator detector. The Cu−Kα lines were used and diagrams were recorded in θ/θ mode, between 5 and 75° (4189 measurements) with a step size of 0.016° in 2θ and a step scan time of 10 s. Given the small amount and low crystallinity of the samples, X-ray powder diffraction diagrams were recorded using an obliquely cut silicon crystal as Zero Background sample Holder (ZBH). Simulation of Y_2Re_2 powder diagram was obtained using Powdercell software considering Cu−Kα lines in a $K\alpha_1/K\alpha_2$ = 0.497 ratio and a Pseudo-Voigt profile of the peaks.

(7) Pointillart, F.; Bernot, K.; Sessoli, R. *Inorg. Chem. Commun.* **2007**, *10*, 471.
(8) (a) DuMez, D. D.; Mayer, J. M. *Inorg. Chem.* **1998**, *37*, 445. (b) Stravropoulos, P.; Edwards, P. G.; Behling, T.; Wilkinson, G.; Motevalli, M.; Hursthouse, M. B. *J. Chem. Soc., Dalton Trans.* **1987**, 169. (c) Libson, K.; Sullivan, J. C.; Mulac, W. A.; Gordon, S.; Deutsch, E. *Inorg. Chem.* **1989**, *28*, 375. (d) Ram, M. S.; Skeens-Jones, L. M.; Johnson, C. S.; Zhang, X. L.; Stern, C.; Yoon, D. L.; Selmarten, D.; Hupp, J. T. *J. Am. Chem. Soc.* **1995**, *117*, 1411. (e) Winkler, J. R.; Gray, H. B. *J. Am. Chem. Soc.* **1983**, *105*, 1373. (f) Brewer, J. C.; Thorp, H. H.; Slagle, K. M.; Brudvig, G. W.; Gray, H. B. *J. Am. Chem. Soc.* **1991**, *113*, 3171.
(9) (a) Bernot, K.; Luzon, J.; Bogani, L.; Etienne, M.; Sangregorio, C.; Shanmugam, M.; Caneschi, A.; Sessoli, R.; Gatteschi, D. *J. Am. Chem. Soc.* **2009**, *131*, 5573. (b) Luzon, J.; Bernot, K.; Hewitt, I. J.; Anson, C. E.; Powell, A. K.; Sessoli, R. *Phys. Rev. Lett.* **2008**, *100*, 247205. (c) Bernot, K.; Luzon, J.; Caneschi, A.; Gatteschi, D.; Sessoli, R.; Bogani, L.; Vindigni, A.; Rettori, A.; Pini, M. G. *Phys. Rev. B* **2009**, *79*, 134419. (d) Chibotaru, L. F.; Ungur, L.; Soncini, A. *Angew. Chem., Int. Ed.* **2008**, *47*, 4126.
(10) Richardson, M. F.; Wagner, W. F.; Sands, D. E. *J. Inorg. Nucl. Chem.* **1968**, *30*, 1275.
(11) Van Bommel, K. J. C.; Verboom, W.; Kooijman, H.; Spek, A. L.; Reinhoudt, D. N. *Inorg. Chem.* **1998**, *37*, 4197.

Physical Measurements. Cyclic voltammetry was performed at room temperature in CH_2Cl_2 on $\mathbf{Dy_2Re_2}$. *n*-$BuNPF_6$ (0.1 M) was used as the supporting electrolyte; glassy carbon as the working electrode; Pt wire and saturated calomel as the counter and reference electrodes, respectively; scan speed = 100 mV s^{-1}. The evaluation of the doping rate of $\mathbf{Dy_xY_{2-x}Re_2}$ was performed by SEM-EDS analysis (Scanning Electron Microscopy-Energy-Dispersive Spectrometry). All observations and measurements were carried out with a JEOL JSM 6400 scanning electron microscope (JEOL Ltd., Tokyo, Japan) with an EDS analysis system (OXFORD Link INCA). The voltage was kept at 9 kV, and the samples were mounted on carbon stubs and coated for 5 min with a gold/palladium alloy using a sputter coater (Jeol JFC 1100). This analysis has been performed by the Centre de Microscopie Electronique à Balayage et microAnalyse (CMEBA) of the University of Rennes (France).

The direct current (dc) magnetic susceptibility measurements were performed on solid polycrystalline sample with a Cryogenic S600 SQUID magnetometer between 2 and 300 K under a magnetic field of 100 Oe for temperatures of 2−65 K, 1 kOe for temperatures of 65−250 K and 10 kOe for temperatures of 250−300 K. These measurements were all corrected for the diamagnetic contribution as calculated with Pascal's constants. The alternating current (ac) magnetic susceptibility measurements were performed using a homemade probe operating in the range 100−25000 Hz.[12] All measurements were performed on pellets to avoid orientation of these very anisotropic materials.

Results and Discussion

Synthesis. The $\mathbf{Re_2Dy_2}$ compound is synthesized according to our previous reported method that was slightly modified. The precursor [ReO(salen)(OMe)] is voluntary dimerized in $\{[Re(salen)]_2O_3\}$ in chloroform under aerobic condition to increase the yield of the coordination reaction. The dimerization of such compounds was previously described by Van Bommel et al.[11,13] The second step consists to put together the $\{[Re(salen)]_2O_3\}$ Lewis bases and $Dy(hfac)_3 \cdot 2H_2O$ Lewis acid in non coordinating solvent (mixture of CH_2Cl_2 and $CHCl_3$) to realize the substitution of one molecule of water by one Re=O moiety.

Cell Determination and X-ray Powder Diagrams. We have previously reported the synthesis and crystal structure of the $\mathbf{Y_2Re_2}$ derivative that is briefly described in this paper.[7] However, we recall here that the crystallization of this complex was rather tricky since the use of both $CHCl_3$ and CH_2Cl_2 (1:1) was mandatory to obtain suitable crystals for X-ray diffraction. These solvents being very volatile, crystals were sealed into glass capillaries to perform a reliable data collection and avoid amorphization. Unfortunately, crystals of the other derivatives ($\mathbf{Gd_2Re_2}$, $\mathbf{Dy_2Re_2}$, and $\mathbf{Dy_xY_{2-x}Re_2}$) rapidly turn into microcrystalline powder and then amorphous compound, even if sealed in a glass capillary. Consequently only the cell determination was performed on these derivatives. The cell parameters are gathered in Table 1 and show that $\mathbf{Re_2Dy_2}$ and $\mathbf{Re_2Y_2}$ are isostructural systems whereas the Gd-based compound crystallizes in a different cell. This is in agreement with the so-called "lanthanide contraction",[14] that underlies the diminution of the ionic radius along the lanthanides series. Hence, a structural change around the gadolinium is often seen and results in non-isostructural families all along the lanthanides series.[15] To confirm the cell determination data and the homogeneity of the sample, X-ray powder diagrams were measured using freshly ground crystals with a fast data acquisition method. All diagrams are superimposed in Figure 2. A simulation of the X-ray powder diagram of $\mathbf{Y_2Re_2}$ was performed using Powdercell software[16] considering the parameters detailed in the Experimental Section. The diagrams of $\mathbf{Y_2Re_2}$, $\mathbf{Dy_2Re_2}$, and $\mathbf{Dy_xY_{2-x}Re_2}$ are highly similar to each other confirming the observation made on crystals, and we are then confident of the isostructurality of $\mathbf{Y_2Re_2}$, $\mathbf{Dy_2Re_2}$, and $\mathbf{Dy_xY_{2-x}Re_2}$ even in their powder form.

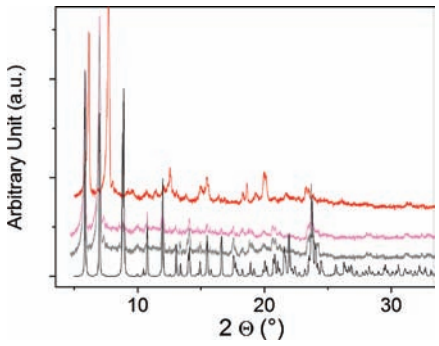

Figure 2. Superposition of X-ray powder diagrams. From bottom to top: (a) Simulation from $\mathbf{Y_2Re_2}$ cif file (black); (b) $\mathbf{Dy_2Re_2}$ (gray); (c) $\mathbf{Dy_xY_{2-x}Re_2}$ (pink); and (d) $\mathbf{Gd_2Re_2}$ (red).

Table 1. Comparison of Cell Parameters of $\mathbf{Y_2Re_2}$, $\mathbf{Gd_2Re_2}$, and $\mathbf{Dy_2Re_2}$

	$\mathbf{Gd_2Re_2}$	$\mathbf{Dy_2Re_2}$	$\mathbf{Y_2Re_2}$
α (deg)	90.297(1)	86.281(4)	86.276(5)
β (deg)	89.694(8)	82.231(4)	82.220(5)
γ (deg)	118.89(2)	82.396(3)	82.396(5)
a (Å)	16.435(1)	12.241(5)	12.222(5)
b (Å)	16.524(4)	12.790(4)	12.783(5)
c (Å)	19.877(1)	15.243(6)	15.222(4)
V (Å^3)	4726.3(20)	2338.9(10)	2332.9 (15)

Structural Description. The $\mathbf{Dy_2Re_2}$ compound crystallizes in the $P\bar{1}$ (No.2) triclinic space group. $\mathbf{Dy_2Re_2}$ can be described as a linear tetranuclear complex composed of two terminal $Dy(hfac)_3(H_2O)$ moieties bridged by the linear central $\{[Re(salen)]_2O_3\}$ entity (Figure 1). The inversion center is localized on the oxygen atom linking the two Re(V) ions. Both terminal Dy(III) ions should adopt a slightly distorted dodecahedral geometry in a DyO_8 environment. In the case of the isostructural $\mathbf{Y_2Re_2}$ tetranuclear compound, the distortion of the dodecahedron can be evaluated with the values of these dihedral angles of 25.7(3), 24.9(2), 27.2(4) and 28.1(3)° compared to the value of 29.5° for a regular dodecahedron. Supporting Information, Figure S1 illustrates the crystal

(12) Midollini, S.; Orlandini, A.; Rosa, P.; Sorace, L. *Inorg. Chem.* **2005**, *44*, 2060.
(13) Reisgys, M.; Spies, H.; Johannsen, B.; Leibnitz, P.; Pietzsch, H.-J. *Chem. Ber./Recueil* **1997**, *130*, 1343.
(14) Cordero, B.; Gomez, V.; Platero-Prats, A. E.; Revés, M.; Echeverria, J.; Cremardes, E.; Barragan, F.; Alvarez, S. *Dalton Trans.* **2008**, 2832.
(15) (a) Daiguebonne, C.; Kerbellec, N.; Guillou, O.; Bünzli, J.-C.; Gumy, F.; Catala, L.; Mallah, T.; Audebrand, N.; Gérault, Y.; Bernot, K.; Calvez, G. *Inorg. Chem.* **2008**, *47*, 3700. (b) Guillou, O.; Daiguebonne, C. Lanthanide ions containing coordination polymers. In *Handbook on the Physics and Chemistry of Rare Earths*; Gschneider, K. A., Bünzli, J.-C.; Pecharsky, V. K., Eds.; Elsevier: Amsterdam, 2005; Vol. *34*, pp 359−404.
(16) Roisnel, T.; Rodriguez-Carjaval *J. Mater. Sci. Forum* **2000**, 118.

packing of the $\mathbf{Y_2Re_2}$ and shows the location of the crystallization solvent molecules. These latter remain in the free space between the complexes and do not interact strongly with the tetranuclear units. This may explain why the crystals so easily lose the CH_2Cl_2 and/or $CHCl_3$ crystallization molecules.

EDS/Elementary Analysis. The Y(III) doping rate in $\mathbf{Dy_xY_{2-x}Re_2}$ has been characterized through EDS measurement. In fact, even if Y(III) and Dy(III) have similar ionic radius and similar chemical properties their effective ratio in the crystal can be significantly different from the one theoretically expected. This is mainly due to the slight differences in hydration and coordination enthalpies along the lanthanide series[15a] that sometimes leads to relevant discrepancies between theoretical and experimental doping rates in such complexes.[17] This technique, coupled with a Scanning Electron Microscope, allows comparing local and global Ln ratios since areas and punctual scans can be performed (Supporting Information, Figure S2). The analysis has been performed on the $\mathbf{Dy_xY_{2-x}Re_2}$ powder and punctual scans on micrometric single crystals give similar Y/Dy ratios than areas scan (100×120 μm). The value of x is determined equal to $x = 0.14$. These two scan types allow us to assert that the doping is homogeneous and no segregation is observed. This is a crucial point when trying then to correlate the magnetic behavior of the complexes to their doping rates.

Electrochemical Properties. The redox properties of $\mathbf{Dy_2Re_2}$ were determined by cyclic voltammetry (Figure 3). For $\mathbf{Dy_2Re_2}$, three quasi-reversible oxidation waves were observed that are not split. This indicates that each oxidation waves corresponds to two-electron events. The two Rhenium ions are simultaneously oxidized. The E^1_{ox}, E^2_{ox}, and E^3_{ox} values are -0.580, $+0.360$, and $+0.860$ mV versus SCE. The first potential corresponds to the reduction of the neutral $\{[Re(V)(salen)]_2O_3[Dy(hfac)_3(H_2O)_2]\}$ complex in the $\{[Re(IV)(salen)]_2O_3[Dy(hfac)_3(H_2O)_2]\}^{2-}$ dianion while the two other ones correspond to the formation of $\{[Re(VI)(salen)]_2O_3[Dy(hfac)_3(H_2O)_2]\}^{2+}$ and $\{[Re(VII)(salen)]_2O_3[Dy(hfac)_3(H_2O)_2]\}^{4+}$ cations, respectively. It is noteworthy that the potentials E^1_{ox} and E^2_{ox} are chemically accessible. In others words, the diamagnetic O=Re(V)−O−Re(V)=O bridge can be reduced or oxidized in paramagnetic O=Re(IV)−O−Re(IV)=O and O=Re(VI)−O−Re(VI)=O bridges, respectively.

Static Magnetic properties. Samples where powder diffraction diagrams are in agreement with $\mathbf{Y_2Re_2}$ simulated diagram are presented here. It is known that diamagnetic ions that bridge organic radical spin carriers can efficiently mediate magnetic exchange interactions.[18] Moreover the energies and the diffuseness of the unoccupied d and vacant p orbitals are expected to have a strong influence on the nature and magnitude of the exchange interaction between the spin carriers.[19] Thus, the diffuse 5d orbitals of Re(V) ions should be efficient in transmitting a magnetic exchange interaction between the two Dy(III) ions in $\mathbf{Dy_2Re_2}$. If one consider the Re_2O_3 bridge, the unoccupied $5d_{xz}$ and $5d_{yz}$ orbitals of the Re(V) ions interact with the filled p_x and p_y orbitals of the terminal and bridging oxygen atoms to give four π-bonding, two π-nonbonding and four π-antibonding molecular orbitals.[20] In total, the bridging Re_2O_3 unit can be described by six delocalized bonding orbitals (two σ and four π). The Re(V) is a $5d^2$ ion, and both electrons are usually localized in the $5d_{xy}$ orbital while the four other 5d orbitals are unoccupied. Consequently the O=Re−O−Re=O central bridge is totally diamagnetic in both $\mathbf{Dy_2Re_2}$ and $\mathbf{Dy_xY_{2-x}Re_2}$ and does not contribute to the susceptibility.

The thermal variation of the magnetic susceptibility for $\mathbf{Dy_2Re_2}$ is shown in Figure 4. The $\chi_M T_{Dy2Re2}(T)$ curve shows a monotonic decrease between 300 and 3 K from

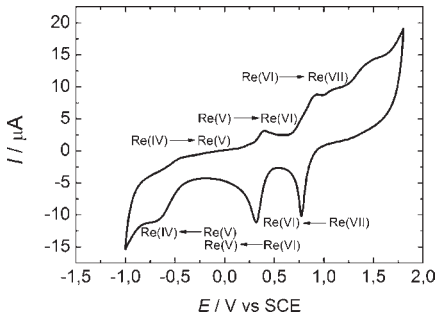

Figure 3. Cyclic voltammetry of $\{[Re(V)(salen)]_2O_3[Y(hfac)_3(H_2O)_2]\}\cdot(CHCl_3)_2(CH_2Cl_2)_2$ $\mathbf{Dy_2Re_2}$ in CH_2Cl_2 at a scan rate of 100 mV s^{-1}.

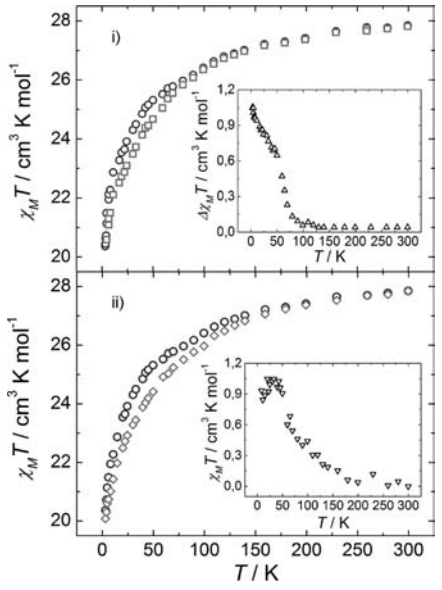

Figure 4. (Top) Thermal variation of the magnetic susceptibility for $\mathbf{Dy_2Re_2}$ (dark gray open circles) and $Dy(hfac)_3\cdot 2H_2O$ (gray squares). In inset, thermal variation of the magnetic susceptibility of $\Delta\chi_M T$(i) = $\chi_M T_{Dy2Re2} - 2\chi_M T_{Dy}$ calculated according to method (i). (Bottom) Thermal variation of the magnetic susceptibility for $\mathbf{Dy_2Re_2}$ (dark gray open circles) and rescaled $\mathbf{Dy_xY_{2-x}Re_2}$ (gray lozenges). In inset, thermal variation of the magnetic susceptibility of $\Delta\chi_M T$(ii) = $\chi_M T_{Dy2Re2} - (2/x)\chi_M T_{DyxY2\text{-}xRe2}$ ($x = 0.18$) calculated according to method (ii).

(17) Poneti, G.; Bernot, K.; Bogani, L.; Caneschi, A.; Sessoli, R.; Wernsdorfer, W.; Gatteschi, D. *Chem. Commun.* **2007**, 1807.

(18) (a) Barclay, T. M.; Hicks, R. G.; Lemaire, M. T.; Thompson, L. K. *Inorg. Chem.* **2001**, *40*, 6521. (b) Oshio, H.; Watanabe, T.; Ohto, A.; Ito, T.; Nagashima, U. *Angew. Chem., Int. Ed. Engl.* **1994**, *33*, 670. (c) Oshio, H.; Ohto, A.; Ito, T. *Chem. Commun.* **1996**, 1541. (d) Benelli, C.; Caneschi, A.; Gatteschi, D.; Pardi, L.; Rey, P. *Inorg. Chem.* **1989**, *28*, 3230. (e) Pointillart, F.; Train, C.; Herson, P.; Marrot, J.; Verdaguer, M. *New J. Chem.* **2007**, *31*, 1001.

(19) Brook, D. J. R.; Abeyta, V. J. *Chem. Soc., Dalton Trans.* **2002**, 4219.

(20) Machura, B. *Coord. Chem. Rev.* **2005**, *249*, 591.

27.85 at room temperature to 20.37 cm^3 K mol^{-1} at 3 K. The $\chi_M T_{Dy2Re2}$ value at 300 K is in agreement with the expected value of 28.34 cm^3 K mol^{-1} for two magnetically isolated Dy(III) ions.[21] We remind that the free Dy(III) ion has a $^6H_{15/2}$ ground state characterized by $g_J = 4/3$.[22] The multiplet is split in zero field in levels separated by a small energy (few hundred cm^{-1}).[21] Consequently the excited sublevels depopulate as the temperature is lowered, and a $\chi_M T$ curve can decrease even in absence of magnetic exchange interaction. That is why one cannot ascribe the decrease of the $\chi_M T_{Dy2Re2}(T)$ curve to a Dy−Dy interaction. To solve this problem, two methods can be explored to cancel the crystal field contribution to $\chi_M T$:(i) the use of a Dy(III) monomeric analogue, and (ii) a Dy(III) doping of a diamagnetic analogue (i.e., **Y_2Re_2**).[4f,17,23]

The $Dy(hfac)_3 \cdot 2H_2O$ precursor has been chosen as the Dy(III) monomeric analogue to estimate J_{Dy-Dy} thanks to method (i). In fact it presents a crystal field equivalent to the one of **Dy_2Re_2**.[23g] By measuring the $\chi_M T$ product of $Dy(hfac)_3 \cdot 2H_2O$ one can thus subtract the crystal field contribution to $\chi_M T$ of Dy(III) in a DyO_8 environment. The $\chi_M T_{Dy}(T)$ curve for the precursor is depicted in Figure 4 (top). $\Delta\chi_M T$(i) is defined by the following expression: $\Delta\chi_M T(i) = \chi_M T_{Dy2Re2} - 2\chi_M T_{Dy}$, $\Delta\chi_M T$(i) can be considered free of single ion effects and thus representative of the nature of the exchange interaction between the Dy(III) ions (inset of the Figure 3). The $\Delta\chi_M T$(i) product takes a constant value of almost 0 cm^3 K mol^{-1} in the 300−100 K temperature range and increases for lower temperatures until a maximum value of 1.05 cm^3 K mol^{-1}.

Concerning the method (ii), a suitable diamagnetic analogue is **Y_2Re_2** since Y^{III} has a $4d^0$ diamagnetic ground state and contrary to what is observed on Eu^{III} doped samples, it does not possess any thermally accessible magnetic excited states.[24] Moreover, the choice of this ion guarantees the isostructurality of the complex (see above). The room temperature $\chi_M T$ value (2.60 cm^3 K mol^{-1}) is in good agreement with the expected doping rate determined through EDS analysis (**$Dy_xY_{2-x}Re_2$**, $x = 0.14 \pm 0.05$) with $x = 0.18 \pm 0.10$. Assuming a random distribution of the lanthanide ions in the doped compound, Dy−Y and Dy−Dy pairs represent 29.50% and 3.25%, respectively. The effect of the magnetic exchange interaction between the Dy^{III} is thus negligible in the doped sample. We have extracted the difference curve $\Delta\chi_M T$(ii) as $\Delta\chi_M T(ii) = \chi_M T_{Dy2Re2} - (2/x)\chi_M T_{DyxY2\text{-}xRe2}$, with $x = 0.18$.[23g] The $\Delta\chi_M T$(i) product increases continually from 0 cm^3 K mol^{-1} at room temperature to 1.05 cm^3 K mol^{-1} at low temperature. The low temperature increase of the $\Delta\chi_M T(T)$ curves, obtained from both method (i) and (ii), indicates a weak but significant ferromagnetic interaction between the Dy(III) ions through the linear and diamagnetic O═Re−O−Re═O bridge although the intrinsic limitations of the two methods make it unrealistic to extract a quantitative value of the Dy−Dy interaction.

Although dipolar interactions have been found to overwhelm exchange ones in a linear Dy_3 cluster,[25] the large separation between the Dy ions (about 12.00 Å) through the penta-atomic bridge allows us to exclude that the observed ferromagnetic interaction is solely due to dipolar interactions.

ac Magnetic Measurements. Dynamic magnetic measurements were performed on the same pellets as for the static ones. In-phase (χ_M') and out-of phase (χ_M'') components of the susceptibility were recorded using 12 logarithmic spaced frequencies in the range 100−15000 Hz. **Dy_2Re_2** is the only derivative presented here since the doping rate of **$Dy_xY_{2-x}Re_2$** is so low that no reliable information can be extracted from its ac measurements. As for numerous lanthanide-based complexes in the absence of external field, the out-of phase signal was almost undetectable.[4f,17] It has been shown that this behavior can be due to zero-field fast tunneling of the magnetization,[3b,26] and the application of a small external field in usually sufficient to partially suppress this fast tunneling.[27] Indeed the field dependence of the susceptibility was recorded, and, as predicted, a strong field dependence of χ_M'' is observed (Supporting Information, Figure S3). The slowest relaxation time is observed for an external field of 700 Oe. This field is thus supposed to be the most efficient one to suppress the zero-field fast tunneling in **Dy_2Re_2** and is then used for the analysis of the dynamic behavior of the complex in the 1.6−8 K range.

The temperature dependence of χ_M' and χ_M'' plotted against the frequency is depicted in Figure 5 (for clarity only the lowest temperature, in the range 1.6−3.2 K, are represented). Same data, but plotted versus temperature, can be found in Supporting Information, Figure S4. Frequency dependence of the out-of-phase component of the susceptibility (χ_M'') is seen for temperature as high as 5 K (Supporting Information, Figure S4), but a reliable extraction of dynamical parameters has been possible only between 1.6 and 2.7 K, the relaxation being too fast for higher temperatures. At a first glance the χ'' versus frequency curve shows a monotonic behavior but a close examination of the low temperature region shows that two regimes are present. In fact, at the three lowest

(21) Kahn, O. *Molecular Magnetism*; VCH: Weinhem, 1993.
(22) Benelli, C.; Gatteschi, D. *Chem. Rev.* **2002**, *102*, 2369.
(23) (a) Kahn, M. L.; Sutter, J.-P.; Golhen, S.; Guionneau, P.; Ouahab, L.; Kahn, O.; Chasseau, D. *J. Am. Chem. Soc.* **2000**, *122*, 3413. (b) Chen, W.-T.; Guo, G.-C.; Wang, M.-S.; Xu, G.; Cai, L.-Z.; Akitsu, T.; Akita-Tanaka, M.; Matsushita, A.; Huang, J.-S. *Inorg. Chem.* **2007**, *46*, 2105. (c) Shiga, T.; Ito, N.; Hidaka, A.; Okawa, H.; Kitagawa, S.; Ohba, M. *Inorg. Chem.* **2007**, *46*, 3492. (d) Hamamatsu, T.; Yabe, K.; Towatari, M.; Osa, S.; Matsumoto, N.; Re, N.; Pochaba, A.; Mrozinski, J.; Gallani, J.-L.; Barla, A.; Imperia, P.; Paulsen, C.; Kappler, J.-P. *Inorg. Chem.* **2007**, *46*, 4458. (e) Barta, C. A.; Bayly, S. R.; Read, P. W.; Patrick, B. O.; Thompson, R. C.; Orvig, C. *Inorg. Chem.* **2008**, *47*, 2280. (f) Barta, C. A.; Bayly, S. R.; Read, P. W.; Patrick, B. O.; Thompson, R. C.; Orvig, C. *Inorg. Chem.* **2008**, *47*, 2294. (g) Rinehart, J. D.; Harris, T. D.; Kozimor, S. A.; Bartlett, B. M.; Long, J. R. *Inorg. Chem.* **2009**, *48*, 3382.
(24) Carlin, R. L. *Magnetochemistry*; Springer: New York, 1986.
(25) Hewitt, I. J.; Lan, Y.; Anson, C. E.; Luzon, J.; Sessoli, R.; Powell, A. K. *Chem. Commun.* **2009**, 6767.
(26) Ishikawa, N.; Sugita, M.; Wernsdorfer, W. *Angew. Chem., Int. Ed.* **2005**, *44*, 2931.
(27) (a) Rebilly, J. N.; Catala, L.; Guillot, R.; Wernsdorfer, W.; Mallah, T. *Inorg. Chem.* **2005**, *44*, 8194. (b) Rebilly, J. N.; Catala, L.; Rivière, E.; Guillot, R.; Wernsdorfer, W.; Mallah, T. *Chem. Commun.* **2006**, 735. (c) Martinez-Lillo, J.; Armentano, D.; De Munno, G.; Wernsdorfer, W.; Julve, M.; Lloret, F.; Faus, J. *J. Am. Chem. Soc.* **2006**, *128*, 14218. (d) Martinez-Lillo, J.; Armentano, D.; De Munno, G.; Wernsdorfer, W.; Clemente-Juan, J. M.; Krystek, J.; Lloret, F.; Julve, M.; Faus, J. *Inorg. Chem.* **2009**, *48*, 3027. (e) Ferbinteanu, M.; Kajiwara, T.; Choi, K.-Y.; Nojiri, H.; Nakamoto, A.; Kojima, N.; Cimpoesu, F.; Fujimura, Y.; Takaishi, S.; Yamashita, M. *J. Am. Chem. Soc.* **2006**, *128*, 9008.

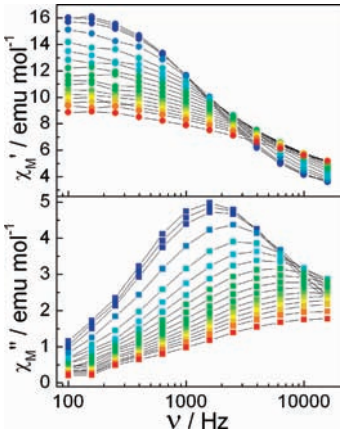

Figure 5. Frequency dependence of the in-phase, χ_M', and out-of-phase, χ_M'', component of the molar susceptibility measured applying a 700 Oe static field for 12 logarithmically spaced frequencies in a 100−16000 Hz range. Color mapping represent temperature varying from 1.6 K (blue) to 3.1 K (red).

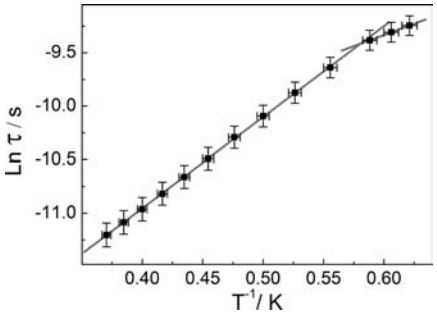

Figure 6. Arrhenius plot and linear regressions that evidence the two dynamic regimes in $\mathbf{Dy_2Re_2}$. Characteristic values are gathered in Table 2.

temperatures (1.60, 1.65, 1.70 K) χ_M'' shows a peak at almost the same frequency. From 1.9 K and above, the χ_M'' trend turns out to be strongly temperature dependent, similarly to what commonly is observed in Dy(III)-based compounds.[4f] At 1.8 K the compound seems to be in between the two regimes.

The characteristic time constants of the system, evaluated as $\tau = (2\pi\nu)^{-1}$, where ν is the frequency at which the maximum of χ_M'' occurs, have been reported in the Arrhenius plot of Figure 6 to evidence the thermal activated character of the relaxation process. Two regimes are observed, and the dynamics parameters summarized in Table 2.

In the high temperature region (1.8−2.8 K), Δ is found equal to 8.52 (±0.55) K, and almost divided by two for the three lowest temperatures (1.6−1.8 K), where Δ = 4.19 (±0.02) K (Table 2). The pre-exponential factors vary from 5.76 (±0.26) × 10^{-7} to 7.13 (±0.10) × 10^{-6} s when passing from the high T to the low T regime (Table 2). This variation of Δ and τ within two regimes has already been seen on single chain magnets,[28] or rather progressively when saturation of the relaxation time because of quantum tunneling of the magnetization is observed on discrete molecules.[17] These dynamic parameters are comparable to what is found on similar compounds even if Δ is smaller in our case.[3d,4] Direct comparison of these

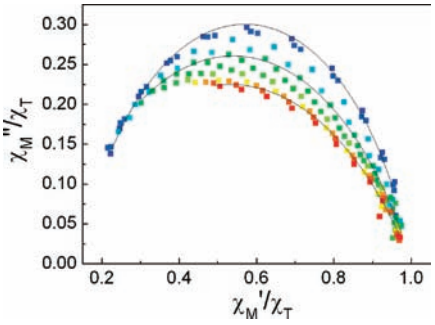

Figure 7. Argand diagram extracted by plotting χ_M' versus χ_M'' and fitted by an extended Debye model (best fits for 1.6 K, 2.0 K, and 2.7 K are depicted). All values are normalized by the isothermal susceptibility (χ_T). Color mapping represent temperature varying from 1.6 K (blue) to 2.8 K (red).

parameters is not possible since they depend on the coordination environment (fully oxygenated or not)[29] and on its geometry. Moreover, it a has been shown that the energy barrier is significantly enhanced if the Dy(III) ions are related by an inversion center,[4f] as it is the case here. This correlation between the parallel anisotropy axes of the Dy(III) is likely to be enhanced when the Rhenium ions will turn paramagnetic and better transmit magnetic exchange interactions.

The two regimes observed in the Arrhenius plot have been found also in the width of the distribution of the relaxation times. To better characterize this distribution an Argand plot has been performed by plotting χ_M'' versus χ_M' (Supporting Information, Figure S5). The curves have been fitted by a Debye model using equation:

$$\chi(\omega) = \chi_S + \frac{\chi_T - \chi_S}{1 + (i\omega\tau)^{1-\alpha}}$$

in which $\chi_T = \chi(\omega \rightarrow 0)$ is the isothermal susceptibility, $\chi_S = \chi(\omega \rightarrow \infty)$ the adiabatic susceptibility, ω the angular frequency of the ac field, and τ the relaxation time of the system at the temperature at which the fit is performed.[30] The α parameter is introduced in the Debye law to characterize the distribution of the relaxation times:[30,31] $\alpha = 0$ corresponds to a unique relaxation time and is thus expected for an ideal SMM.[32] On the contrary $\alpha \rightarrow 1$ characterizes an infinity of relaxation times and is characteristic of spin-glasses.[33] The parameters extracted from the curves in the range 1.6−2.7 are gathered in Supporting Information, Table S1 while the low temperature experimental curves and simulation are shown in Figure 7 by normalizing the χ values against χ_T to allow a better comparison.

In $\mathbf{Dy_2Re_2}$, the three lowest temperatures shows similar α values (0.22, 0.24, 0.24) whereas definitely higher ones are obtained when the temperature is rising (0.31 to 0.39

(28) Bernot, K.; Bogani, L.; Caneschi, A.; Gatteschi, D.; Sessoli, R. *J. Am. Chem. Soc.* **2006**, *128*, 7947.

(29) Pointillart, F.; Bernot, K. *Eur. J. Inorg. Chem.* **2010**, 952.

(30) Cole, K. S.; Cole, R. H. *J. Chem. Phys.* **1941**, *9*, 341.

(31) (a) Dekker, C.; Arts, A. F. M.; Wijn, H. W.; van Duyneveldt, A. J.; Mydosh, J. A. *Phys. Rev. B* **1989**, *40*, 11243. (b) Aubin, S. M. J.; Sun, Z.; Pardi, L.; Krzystek, J.; Folting, K.; Brunel, L.-C.; Rheingold, A. L.; Christou, G.; Hendrickson, D. *Inorg. Chem.* **1999**, *38*, 5329.

(32) Gatteschi, D.; Sessoli, S.; Villain, J. *Molecular Nanomagnets*; Oxford University Press: Oxford, 2006.

(33) Mydosh, J. A. *Spin Glasses: An Experimental Introduction*; Taylor & Francis: London, 1993.

Table 2. Characteristic Δ and Time Constants Extracted from the Analysis of the Dynamic Magnetic Measurements of $\mathbf{Dy_2Re_2}$[a]

	τ_0 (s)	Δ (K)	R1	best α	R2
low *T* regime	7.13 (±0.10) × 10^{-6}	4.19 (±0.02)	0.99998	0.22 (±0.02)	0.98163
high *T* regime	5.79 (±0.26) × 10^{-7}	8.52 (±0.55)	0.99991	0.31 (±0.01)	0.99703

[a] R1 and R2 are the agreement factor of the fittings of the Arrhenius and Argand plot, respectively.

for 1.9 to 2.3 K) (Table 2). Usually the opposite trend is observed for either 3d or 4f based SMMs, with α increasing significantly on approaching the quantum regime. Unfortunately the temperature dependence of α is seldom reported in the literature, and a rationalization of this behavior at the moment is not possible.

Conclusions

In this paper, the 5d4f $\{[Re(salen)]_2O_3[Dy(hfac)_3(H_2O)]_2\}(CHCl_3)_2(CH_2Cl_2)_2$ (**Dy_2Re_2**) tetranuclear complex has been synthesized from the two [ReO(salen)(OMe)] and $Dy(hfac)_3 \cdot 2H_2O$ mononuclear precursors.

Thanks to the diamagnetic doping with Y(III) we have unambiguous evidence that the diamagnetic $[Re(salen)]_2O_3$ bridge is efficient in transmitting a weak ferromagnetic exchange interactions between the terminal Dy(III). Although the magnetization dynamics is affected by a strong tunnelling in zero field, as observed for the most pure lanthanide-based SMM, it should be interesting and informative in the rational design of 4f-5d heterobimetallic SMMs to convert the diamagnetic bridge into a paramagnetic fragment. The electrochemical studies on **Dy_2Re_2** have revealed a rich redox chemistry involving several quasi-reversible oxidation and reduction processes of the Rhenium. Chemical and electrochemical reduction and oxidation of **Dy_2Re_2** are in progress to obtain its paramagnetic analogue with Re(IV) or Re(VI) ions. Such strategy has been successful for the mono,[34] bi,[35] and tri-electron[36] reduction of the Mn12 SMM. Moreover, the remaining water molecule on the $Dy(hfac)_3(H_2O)$ unit offers a labile position which, coordinated by suitable ligands, may give rise to extended magnetic structures.

Acknowledgment. We acknowledge financial support from Italian MURST (FIRB and PRIN grants), from the EC through the Human Potential Program RTN-QUELMOLNA (MRTN-CT-2003-504880), from the NE-MAGMANET (NMP3-CT-2005-515767), and F.P. thanks German DFG (SPP1137) for his postdoctoral fellowship. Yann Le Gal and Isabelle Péron (CMEBA) are acknowledged for the cyclic voltammetry measurements and Scanning Electron Microscopy-Energy-Dispersive Spectrometry Analysis, respectively.

Supporting Information Available: Crystal packing of **Ln_2Re_2** (Figure S1), SEM images and EDS analyses of **$Dy_xY_{2-x}Re_2$** (Figure S2), Field dependence of the out-of phase χ_M'' (Figure S3), $\chi_M'(T)$ and $\chi_M''(T)$ curves (Figure S4), Argand diagram (Figure S5), and α values (Table S1) for **Dy_2Re_2**. This material is available free of charge via the Internet at http://pubs.acs.org.

(34) (a) Schake, A. R.; Tsai, H.-L.; de Vries, N.; Webb, R. J.; Folting, K.; Hendrickson, D. N.; Christou, G. *J. Chem. Soc., Chem. Commun.* **1992**, 181. (b) Eppley, H. J.; Tsai, H. L.; Devries, N.; Folting, K.; Christou, G.; Hendrickson, D. N. *J. Am. Chem. Soc.* **1995**, *117*, 301. (c) Wernsdorfer, W.; Chakov, N. E.; Christou, G. *Phys. Rev. Lett.* **2005**, *95*, 037203.

(35) (a) Soler, M.; Chandra, S. K.; Ruiz, D.; Huffman, J. C.; Hendrickson, D. N.; Christou, G. *Polyhedron* **2001**, *20*, 1279. (b) Soler, M.; Wernsdorfer, W.; Abboud, K. A.; Huffman, J. C.; Davidson, E. R.; Hendrickson, D. N.; Christou, G. *J. Am. Chem. Soc.* **2003**, *125*, 3576.

(36) Bagai, R.; Christou, G. *Inorg. Chem.* **2007**, *46*, 10810.